



Spatial and temporal variations in surface snow chemistry along a traverse from Dome C toward South Pole in the framework of East Antarctic International Ice Sheet Traverse (EAIIST) project.

5 Simone Ventisette¹, Samuele Baldini¹, Claudio Artoni², Silvia Becagli^{1,3}, Laura Caiazzo^{1,4}, Barbara Delmonte², Massimo Frezzotti⁵, Raffaello Nardin¹, Joel Savarino⁶, Mirko Severi^{1,3}, Andrea Spolaor³, Barbara Stenni⁷, and Rita Traversi^{1,3}.

¹Department of Chemistry “Ugo Schiff”, University of Florence, Sesto Fiorentino, Florence I-50019, Italy

²Department of Environmental Science, University of Milano-Bicocca, Milan, Italy

³Institute of Polar Sciences, ISP-CNR, University of Venice, V. Torino 155, 30172 Venice-Mestre, Italy

10 ⁴Laboratory for Observations and Measurements for Environment and Climate (SSPT-PROTER-OEM), ENEA C.R. Casaccia, 00123, Roma, Italy

⁵Department of Science, University of Roma Tre, Largo S. Leonardo Murialdo, 1, 00146, Roma, Italy.

⁶Institut des Géosciences de l’Environnement, Université Grenoble Alpes, CNRS, IRD, Grenoble INP, 38400 Grenoble, France

15 ⁷Ca’Foscari University of Venice, Department of Environmental Sciences, Informatics and Statistics, Via Torino 155, 30172 Venice Mestre, Italy.

Correspondence to: Silvia Becagli (silvia.becagli@unifi.it)

Abstract. As part of the “East Antarctic International Ice Sheet Traverse” (EAIIST) project, 6 cm surface snow and snow pit samples (until about 2 m depth) were collected along a traverse from Dome C toward the geographic South Pole during the 20 2019-2020 Antarctic campaign. Results on spatial distribution of major ions are here reported to understand deposition and post deposition processes in sites with very low snow accumulation rate in the East Antarctic Plateau where megadune and wind crust areas are present.

The volcanic signature of Pinatubo eruption (occurred in 1991) was clearly visible in the non-sea salt SO_4^{2-} stratigraphy from two snow pits (AGO-5 and PALEO) allowing the determination of annual accumulation rates that revealed to be 25.7 and 22.6 25 mm of water equivalent/year, respectively at the two sites. Moreover, a decreasing trend in accumulation rate as the distance from the Indian Ocean increases was detected. Mineral dust concentration and size show presence of a criptotephra layer in AGO5 and PALEO stratigraphies which is stratigraphically compatible with the deposition of volcanic ash related to the Puyehue-Cordón Caulle explosive eruption occurred in June 2011. The ssNa^+ fraction, accounting for the 92.5% of the total Na^+ , is preserved stably in the snow layers and was chosen as marker of sea spray deposition. Despite the very low 30 accumulation rate in this area, the main deposition process of sea spray aerosol is the wet deposition. Conversely, both biogenic and crustal nssSO_4^{2-} are dry deposited, the total flux of nssSO_4^{2-} resulted to be constant in the Antarctic plateau, but the biogenic to crustal ratio increases as distance from Dome C increases. The presence and quantification (by nssCa^{2+}) of a dry deposited crustal source, as the biogenic one, sheds light on the interpretation of nss SO_4^{2-} biogenic stratigraphy during glacial and interglacial time in Antarctic ice cores. NssCl^- represent the fraction of Cl^- deposited as HCl and arises from the exchange



35 reactions between chloride in the sea salt aerosol and acidic species such as H_2SO_4 and HNO_3 that occurs both into the
atmosphere (in this case HCl is deposited by wet deposition) and into the snow (at the expenses of NaCl or MgCl_2 deposited
as sea salt aerosol). The latter process could be particularly efficient in sites affected by wind crust formation, probably because
of a longer exposure time of the snow layers to the atmosphere favouring the HCl volatilization. Another important marker in
ice core is HNO_3 , that in the considered sites is found at very high concentration in the most superficial 3 cm of snow due to
40 the uptake by superficial snow and possibly concentration effects from the layers beneath, but it is reversibly deposited. The
depth of the active layer for HNO_3 reemission was calculated and it spans from 22 cm to 12 cm; in addition, the concentration
preserved in the snow decreases as the accumulation rate decreases, but wind scouring increases the efficiency of re-emission
processes in the active layer. The knowledge and quantification of all the above reported processes will allow the interpretation
of the ice core stratigraphies in low accumulation site likely hopefully recording, at selected sites, the climate history of more
45 than one million years ago.

1 Introduction

Understanding the spatial and temporal variability of snow chemical composition is a prerequisite in the glaciological and
glaciochemical studies. It allows obtaining reliable information about past variations in the chemical composition of snow
recorded in ice cores, and to evaluate the mass transport of chemical markers, which, due to the high spatial variability in
50 aerosol composition, scavenging processes, snow accumulation and wind distribution, are fundamental to characterize
climatically unexplored area of the Antarctic ice sheet (Becagli et al., 2005; Bertler et al., 2005; Benassai et al., 2005).

Several studies investigated the spatial variation of glaciochemical data across the ice sheet along traverses during the
International Trans-Antarctic Scientific Expedition (ITASE), e.g., Dumont d'Urville Station (DDU) to Dome C, coast-interior
traverse in Adélie Land, Syowa Station to Dome F, Terra Nova Bay to Dome C, Zhongshan Station to Dome A and US ITASE
55 in West Antarctica (Dahe et al., 1992; Dixon et al. 2013; Legrand and Delmas 1985; Mulvaney and Wolff 1994; Proposito et
al. 2002; Shi et al. 2021; Suzuki et al. 2002), but a large part of the Antarctic ice sheet is still unexplored.

In this framework, the EAIIST project (East Antarctic International Ice Sheet Traverse) is an international collaboration aiming
to study the interior of the Antarctic Plateau between the Italian-French "Concordia" station ($75^\circ 06' 01'' \text{ S}$, $123^\circ 20' 48'' \text{ E}$)
and the geographic South Pole. The general objective of the project is to study the Antarctic ice sheet in its most arid and
60 unknown places, which presents unique and extraordinary surface morphological characteristics. Indeed, the sampled area has
a high orographic interest containing several unique geographical features such as "megadune" or "wind crusts" area,
accompanied by physical and chemical processes of the snowpack such as post-depositional variations that are not yet fully
understood. Besides, despite the formation of wind crusts had been accurately studied by field observations and wind tunnel
experiments (e.g. Sommer et al., 2018), its effect on surface mass balance, isotopic and chemical composition is still poorly
65 understood.



This study presents chemistry data from 6 cm surface snow samples and about 2 m depth snow pits collected along the EAIIST Concordia Station to South Pole 2019-20 traverse. We use these data to determine the spatial variability of chemical deposition and post deposition processes over an inaccessible area of the Antarctic continent. Besides, as this area is characterized by extremely low accumulation rate and extensively recrystallized snow, we use the chemical variation as function of space and depth to further infer surface and sub-surface conditions along the traverse route.

2 The studied area

The surface snow and snow-pit samples were collected during the 2019-2020 Antarctic campaign, in an area of the East Antarctic Plateau that was crossed by the scientific traverse carried out in the framework of the EAIIST project (Fig. 1).

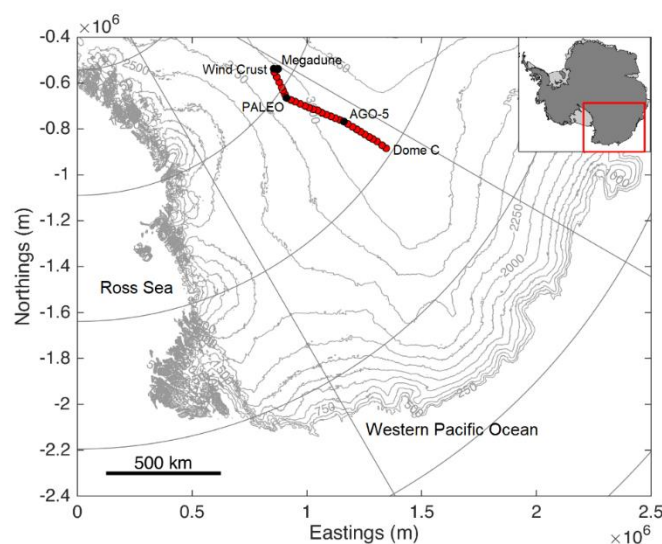


Figure 1. Map of Antarctica with the sampling sites. Superficial snow sampling sites of the EAIIST traverse are reported in red. The sites in which snow pit samples were collected are reported in black. Dome C, where Concordia Station is located, is also reported on the map as a reference point.

The route started from Dome C and closely followed the 123°E Meridian with small variations in altitude, which remains close to 3000 m a.s.l. (3061 ± 116 m) for the whole traverse (Fig. 2a and Table 1S) to minimize the variability in the composition of the snow due to the altitude variations. It has been shown, in fact, that the concentrations of dissolved components in the snow change in relation to several intrinsic parameters of the sampling site such as the distance from the sea, the altitude and the accumulation rate (Becagli et al. 2004; Bertler et al. 2005; Khodzher et al. 2014; Proposito et al. 2002; Udisti et al. 2004).

The distance from the Indian Ocean increases as the distance from Dome C increases, conversely the distance from Ross Sea decreases making quite constant the distance from the nearest ocean. Indeed, previous studies shown that the main part of the



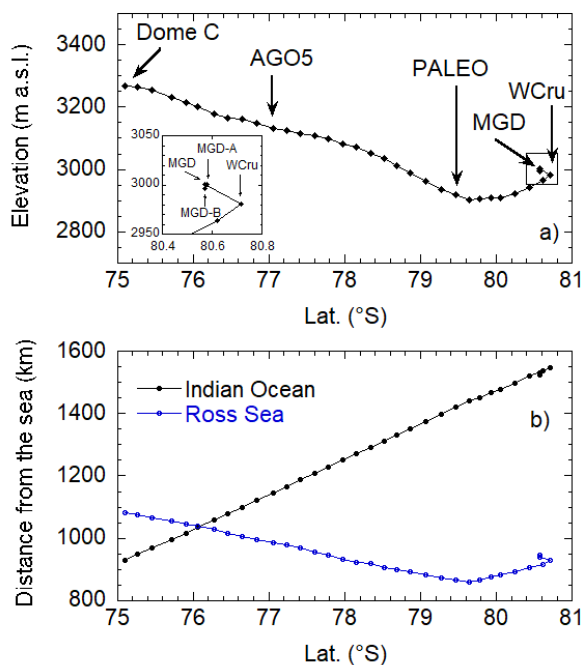
sampled sites mainly receive air masses from the Indian Ocean and only the few farthest sites from Dome C are affected also by air masses coming from the Ross Sea (Scarchilli et al., 2011; Sodemann and Stohl, 2009).

The traverse crosses areas of the ice sheet characterized by the presence of wind crust and megadunes. Megadune fields occupy large areas in the interior of the East Antarctic ice sheet and are the result of peculiar snow accumulation and redistribution processes. These areas are usually characterized by slightly steeper regional slope and the presence of highly persistent katabatic winds. Megadunes are characterized by an amplitude of 2 to 4 m with a wavelength ranging from 2 to 5 km. Their net accumulation differs from the adjacent non-megadune areas from 25% (leeward or erosion faces) to 120% (windward or accumulation faces). Erosion faces are characterized by glazed, sastrugi-free surfaces and extensive hoar formation whilst accumulation faces are covered by large rough sastrugi up to 1.5 m in height (Frezzotti et al., 2002; Traversa et al., 2023).

90 processes. At five sampling sites, named AGO-5, PALEO, Wind Crust (WCru), Megadune Erosion (MGD-E), and Megadune Accumulation (MGD-A), additional snow-pits sampling was conducted.

95 At five sampling sites, named AGO-5, PALEO, Wind Crust (WCru), Megadune Erosion (MGD-E), and Megadune Accumulation (MGD-A), additional snow-pits sampling was conducted.

The list of sampling sites together with geographical characteristics and the type of sampling performed are reported in Table 1S.



100 **Figure 2.** Elevation (plot a) and distance from the sea (plot b) respect to the latitude for each sampling sites. The sampling points where snow pits were dug (AGO5, PALEO, WCru, MGD-A and MGD-E) are reported in plot a. The detail of MGDs and WCru area is reported as enlarged square inside plot a.



3 Methods

3.1. Sampling procedures

105

All samples were collected using 50 mL polyethylene Corning® tubes by personnel wearing low particulate release clothing, polyethylene gloves (over silk thermal gloves) to minimize external contamination. Surface snow samples (uppermost 6 cm of snow) were collected by directly inserting the tubes into the surface snow of the sampling site (upwind and at a sufficient distance from the convoy to reduce the contamination risk). The density of the surface snow was determined by inserting a stainless-steel cylinder open on two sides in the snow; the recovered (known) volume of snow was stored in a plastic bag and weighed in the convoy's cold laboratory.

110

In the above mentioned 5 sites about 2 m snow-pit were dig and samples were collected using the following procedure: first, the surface wall of the pit was decontaminated after the excavation by removing approximately 20 cm of the vertical layer with a plastic scraper. Subsequently, Corning® tubes were inserted one below the other into the vertical wall, collecting samples at a resolution of 30 mm (the diameter of the tube).

115

After sampling, the tubes were put in their rack, sealed in polyethylene bag, and kept at -20°C throughout transport and up to the time of analysis. Any interaction with the samples was performed within a clean room (Class 10000), wearing low particle release clothing. Samples were left thawing at room temperature just before the analysis inside a class 100 laminar flow hood, in the same tube in which they were collected.

120

3.2 Analysis

For each sample, the cationic (Na^+ , NH_4^+ , K^+ , Mg^{2+} , Ca^{2+}) and anionic (Cl^- , NO_3^- , SO_4^{2-}) content was determined by Ion Chromatography using an integrated system of two ion chromatographs working in parallel. A new method was optimized and applied to these samples allowing to obtain fast (5.50 minutes) and high sensitivity measurements without compromising resolution between chromatographic peaks. The risk of contamination during the sample loading was minimized by using an autosampler (222XL Liquid Handler, Gilson, Middleton, WI, USA) with a single steel needle connected to a peristaltic pump (Gilson Minipuls 3) remotely controlled (Morganti et al., 2007).

125

For anions determination, samples were loaded into a ThermoFisher - Dionex Ion Pac TAC-2 (3 x 35 mm) by a peristaltic pump with an average flow rate of 1.30 mL/min for 0.75 minutes, corresponding to 0.975 mL of sample loaded into the TAC. A ThermoFisher Dionex DX500 ion chromatograph (Sunnyvale, CA, USA) equipped with a Dionex Ion Pac AS4A 4 x 25 mm (10-32) analytical column and a Dionex AERS 500 self-regenerating conductivity suppressor (4 mm) was used for anions determination. Chromatographic peaks were detected by a Dionex CD25 conductivity detector, which uses the eluent stream leaving the detector as a regenerating solution. An isocratic run was performed using a 2.0 mM/3.0 mM $\text{NaHCO}_3/\text{Na}_2\text{CO}_3$ as

130



135 eluent with a 2.0 mL/min flow. In these condition organic anions (Acetate, Formate, and Methanesulfonate) are not detectable as they lie in the water dip, but they are separate from Chloride peak and do not affect its determination.

The determination of the cationic content was obtained using a Dionex ICS 1000 ThermoFisher ion chromatograph equipped with a Dionex CERS 500 self-regenerating conductivity suppressor (4 mm, suppression current 180 mA) and a Dionex DS6 conductivity detector. Thanks to the low concentration of the ions and the absence of other ions interference, separation was
140 obtained using two Dionex CG12 guard columns (4 x 50 mm) that allow obtaining an excellent peak resolution in a shorter total run time than using a single separation column. Isocratic run with 12.5 mN H₂SO₄ sample injection as eluent at flow, 2.0 mL/min was used. Besides, the low retention time for all the ions allow obtaining high and narrow peaks, therefore increasing the sensitivity of the measurements that are obtained by the injection of only 200 µL of sample.

Dionex Chromeleon® chromatography software was used for instrumentation control and data acquisition.

145 External 5-point calibration curves were used for quantitative determination of each ion, standard solutions for calibrations were prepared daily diluting 1000 mg/L Merck standard solutions (Darmstadt, Germany) with MilliQ ultrapure water (Resistivity > 18 MΩ·cm).

Detection limits (d.l.) and reproducibility are reported in Table 1.

150 **Table 1.** Detection limit and reproducibility (%) for each ion. Detection limits are obtained as the concentration corresponding to a signal of three times the standard deviation of 10 repetitions of a 10 µg/L standard solution.

Ion	d.l. (mg/L)	Repr. (%)
Cl ⁻	4.9	3.4
NO ₃ ⁻	3.0	2.7
SO ₄ ²⁻	2.1	1.3
Na ⁺	0.1	1.9
NH ₄ ⁺	0.6	3.8
K ⁺	0.3	2.9
Mg ²⁺	0.2	1.6
Ca ²⁺	0.2	1.9

Blanks were evaluated before and after each calibration procedure resulting below the detection limit for each determined ion. Within the same snow pits dug for chemical sampling, a parallel line of samples was dedicated to mineral dust samples. These
155 were analyzed at the EUROCOLD Laboratory of Milano-Bicocca in clean room ISO6 by means of a Beckman Coulter Multisizer 4e equipped with a 30 µm orifice tube, following the standard analytical protocol for dust analyses in ice cores (Delmonte et al., 2004).



4. Results and discussion

4.1 Sea-salt and non-sea-salt fractions

160 It is well known that Na^+ and Ca^{2+} have both sea spray and crustal sources, therefore sea-salt (ss) and non-sea-salt (nss) fraction of both ions was calculated using a simple two-equations system (Röthlisberger et al. 2002; Udisti et al. 2012)

$$\text{ssNa}^+ = \text{Na}^+ - 0.562 \cdot \text{nssCa}^{2+} \quad (\text{equation 1})$$

$$\text{nssCa}^{2+} = \text{Ca}^{2+} - 0.038 \cdot \text{ssNa}^+ \quad (\text{equation 2})$$

165

where $0.562 = \text{Na}^+/\text{Ca}^{2+}$ (w/w) in the crust (Bowen 1979) and $0.038 = \text{Ca}^{2+}/\text{Na}^+$ (w/w) in seawater (Bowen 1979).

The sea salt represents the dominant contribution to Na^+ concentration, accounting for the 92.5% of the total Na budget measured in superficial snow in all the sampled sites in this area. SsNa^+ concentration was chosen to assess the contribution of sea salt aerosol for the other ions present in the sea water (Mg^{2+} , K^+ , Ca^{2+} and Cl^-). The correlation plots of these ions respect to SsNa^+ show for Mg^{2+} and K^+ a dominant sea salt source demonstrated also by a good correlation with SsNa^+ ($R^2 > 0.8$) and ratios with SsNa^+ close to the sea water ratios (Fig. 1Sa e b). Due to Ca^{2+} crustal source, for this ion a worse correlation than K^+ and Mg^{2+} , and a slope of the regression line higher than $(\text{Ca}^{2+}/\text{Na}^+)$ sea water ratio was found (Fig.1Sc). Indeed, by the equation 1 and 2 is possible to estimate the nssCa^{2+} contribution that as average represents the main contribution (77.6%) of total calcium budget.

175 In the case of Cl^- , a correlation with SsNa^+ was found, but all (except one) samples have a Cl^-/Na^+ ratio higher than sea water one. This suggests the presence of an alternative source for this ion.

HCl can arise by the interaction between sea spray particles (containing NaCl and MgCl_2) and some acidic species (mainly HNO_3 and H_2SO_4 ; reaction 1 and 2 respectively). The volcanic source of HCl can be excluded due to its sporadic and extreme character.

180



185 These acid-base exchange reactions produce gaseous HCl, which follows different transport and deposition pathways than the sea-spray particles (Kerminen et al., 2000; McInnes et al. 1994). The amount of Cl^- present in snow layer as HCl (nssCl^- or excCl^-) can be calculated using the following equation:

$$\text{nssCl}^- = \text{Cl}^- - \text{ssNa}^+ \cdot (\text{Cl}^-/\text{Na}^+)_{\text{sw}} \quad (\text{equation 4})$$

190



where Cl^- and ssNa^+ are the total Cl^- and sea-salt Na^+ concentration. $(\text{Cl}^-/\text{Na}^+)_{\text{sw}}$ is the Cl^- to Na^+ ratio in sea water which is 1.81 w/w (Bowen 1979). Using this equation is possible to highlight that in superficial snow the fraction of Cl^- present as HCl is on average the 46% .

The ssNa^+ was also used to calculate the non-sea salt sulphate fraction (nssSO_4^{2-}) using the following equation:

195

$$\text{nssSO}_4^{2-} = \text{tot SO}_4^{2-} - 0.25 * \text{ssNa}^+ \quad (\text{equation 5})$$

where 0.25 is the $\text{SO}_4^{2-}/\text{Na}^+$ ratio in sea water (Bowen 1979). The value of $\text{SO}_4^{2-}/\text{Na}^+$ in sea water was used instead of the $\text{SO}_4^{2-}/\text{Na}^+$ ratio of 0.09 (w/w) characteristic of sea-salt aerosol arising from frost flowers (Legrand et al., 2017) as the latter source was demonstrated to be significant only for winter samples and has a minor impact respect to the open ocean source to the annual budget (Legrand et al., 2017; Udisti et al., 2012). Anyway, the impact of sea salt SO_4^{2-} is very low in this area, accounting as average only for 12.4% of total sulphate. This value agrees with previous data obtained in the Antarctic Plateau (Khodzher et al. 2014; Li et al. 2016; Shi et al. 2021; Traversi et al. 2004; Uemura et al. 2016), showing that the the main source of SO_4^{2-} is from secondary sources. Previous studies by sulfur isotopic measurements show that the contribution of biogenic source (from oxidation of phytoplanktonic dimethylsulphide) in Antarctica is largely dominant over the other sources of sulfate (Khodzher et al. 2014; Uemura et al. 2016). The volcanic source of nssSO_4^{2-} (from oxidation of volcanic SO_2) is sporadic, in correspondence of volcanic eruption and it is well evident in central Antarctic Plateau as concentration spikes of nssSO_4^{2-} superimposed to the biogenic background (Castellano et al. 2005). The presence of sulfate spikes ascribable to historical know volcanic eruptions allows obtaining the dating of the snow layers and to assess the accumulation rate.

210

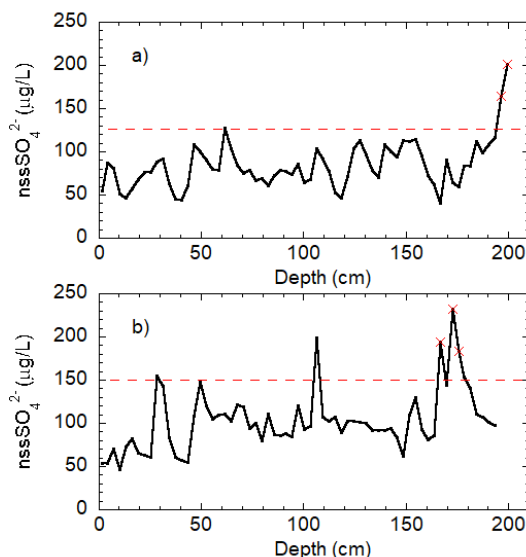
4.2 Volcanic stratigraphy and accumulation rate trend

Due to the very low accumulation rate in all the sampled sites the stratigraphic dating of snow layer is unpracticable. Therefore, the identification of volcanic signatures in the snow pit sulfate stratigraphies is used to calculate the accumulation rate. Since volcanic eruptions emit (amongst other components) large amount of SO_2 in the atmosphere, if the volcanic eruption is sufficiently strong, SO_2 is able to reach the stratosphere and it can have hemispheric distribution. Therefore, it is possible to identify past volcanic eruptions in snow layers occurred at least in Southern hemisphere (but also until 20°N), as concentration spikes of nssSO_4^{2-} arising from the stratospheric oxidation of SO_2 and subsequently deposition on the Antarctic plateau. These concentration spikes are superimposed to the biogenic background and can be statistically recognizable from the background values (Castellano et al., 2005). By matching these volcanic signatures with historical records or other already dated cores, it is possible to date ice records (Castellano et al., 2005; Severi et al., 2007; Nardin et al., 2020).

To highlight the volcanic source an iterative method from Castellano et al. (2005) was adopted, consisting in calculating a nssSO_4^{2-} background from biogenic source and looking for at least two consecutive samples with nssSO_4^{2-} concentration overcoming the background + 2σ . The volcanic eruption of the Pinatubo occurred in 1991 CE and recorded in Antarctic snow



225 layer in 1992 CE deposition (Cole-Dai and Mosley-Thompson, 1999) can be found in the AGO-5 and PALEO records at the depths 199.5 cm and 172.5 cm respectively (Fig. 3). By taking into account the snow density of the snow pits layers, the mean accumulation rates for the 1992-2019 period at the two sites were estimated to be 25.7 and 22.6 mm of water equivalent/year respectively.



230 **Figure 3.** NssSO₄²⁻ stratigraphies for AGO-5 (a) and PALEO (b) snow pits. The volcanic threshold obtained by the iterative method is shown as a red dashed horizontal line. Sample points ascribed to a volcanic signature are highlighted as red crosses.

To increase the reliability of accumulation rate obtained by the only signature of Pinatubo eruption the insoluble particle stratigraphy obtained at AGO5 and PALEO were compared to find dust events recorded at both sites.

235 The concentration profiles of insoluble particles obtained for AGO5 and PALEO snow pits show background dust concentration levels around 15 ppb at both sites. Superimposed to background, AGO5 shows a 18 cm-broad peak in the mineral dust concentration record from about 55.5 cm depth to 73.5 cm depth (Fig. 4), when concentration levels rise to ca. 4 times above background; similarly, the PALEO snowpit stratigraphy shows a 15-cm wide peak between 34.5 and 49.5 cm depth, when concentrations rise to ~5 times background levels, on average. Within both peaks it is possible to observe that

240 mineral dust grain size progressively decreases since the beginning of the event, or initial dust rise, until a minimum centred around 61.5-64.5 cm depth at AGO5 and 37.5-40.5 cm at PALEO, when the modal values of the dust grain size distribution decrease below the typical background levels of ca. 2 µm. The Weibull functions used to fit dust spectral data of volume-size distributions at both sites show modal values as low as 1.73 (±0.02) µm for AGO5 and 1.70 (±0.02) µm for PALEO (Fig 5) at the time of dust size minima occurring when the Coarse Particle Percentage (CPP%) drops to -10% with respect to background

245 (arrows in Fig.4). Both events are associated with an almost concomitant increase in nssSO₄²⁻ concentration even if the nssSO₄²⁻ values lie in the variability range of biogenic background. All these peculiar features are typical of cryptotephra layers (Narcisi



et al., 2019; Delmonte et al., 2004) occasionally found in Antarctic snow. Therefore, we believe that these two peaks represent the same volcanic event preserved in the snowpack, which can be used as additional relative chronostratigraphic marker between the two snow pits. The stratigraphic location of the peak is compatible with deposition of volcanic ash from the Puyehue-Cordón Caulle (Chile) explosive eruption event of June 2011 detected also in West Antarctica (Koffmann et al., 2017), although glass geochemistry is necessary to unequivocally infer the volcanic source.

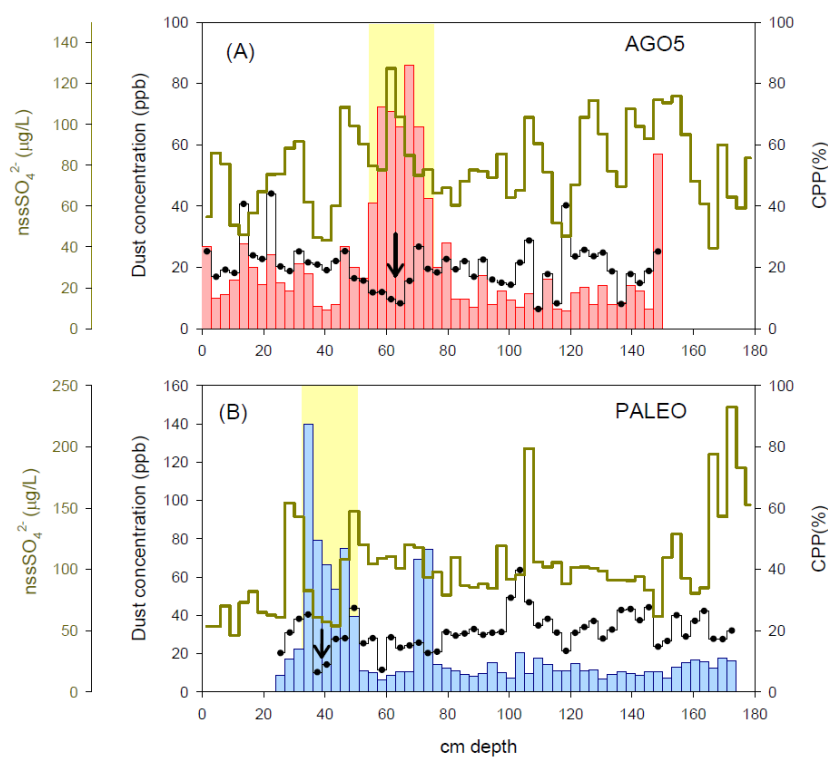
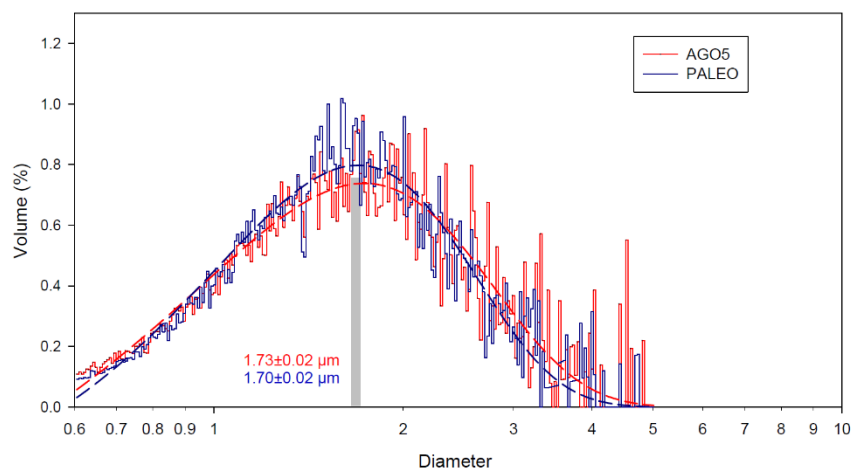


Figure 4. Dust concentration profile for the AGO5 (plot A) and PALEO (plot B) snow pits (ppb, or ng of dust per mL of sample), with the nssSO_4^{2-} profile and the Coarse Particle Percentage (CPP, %) index (Delmonte et al., 2004) on the right axis. The black arrow indicates the dust size minimum. nssSO_4^{2-} concentrations are shown by the green step line, dust concentrations by pink columns and CPP (%) by black circles and interpolating black line. Yellow shadowed areas mark dust concentration peaks.



260

Figure 5: Dust volume (mass)-size distribution for AGO5 and PALEO samples corresponding to the layers of dust size minima indicated by arrows in figure 4. For both spectra, the dust mode has been calculated through a 4-parameter Weibull distribution used to fit data. Modal values are almost identical, i.e. $1.73 (\pm 0.02) \mu\text{m}$ for AGO5 and $1.70 (\pm 0.02) \mu\text{m}$ for PALEO site.

265

Comparing the values of accumulation rate here assessed with the values estimated at Dome C obtained by previous studies (Traversi et al., 2009; Caiazza et al., 2021), it is possible to highlight a decreasing trend of accumulation rate as the distance from the Indian Ocean increases (Table 2).

4.3 Deposition and post deposition processes as function of accumulation rate and glaciological features.

270

To understand the deposition and re-emission processes of the analyzed ions is fundamental the study of the concentration and deposition flux trend as function of the sampling site locations that, as above described, differ mainly for accumulation rate, snow redistribution by the winds and eventual wind crust formation.

By using a linear regression to fit the decreasing trend of snow accumulation as distance from the Indian Ocean increases, it was possible to evaluate the accumulation rate for each site and therefore the deposition flux of each ion by the equation:

275

$$F = C \cdot \text{Acc}$$

Where F is the deposition flux ($\mu\text{g}/\text{m}^2 \text{ yr}$), C is the ion concentration ($\mu\text{g}/\text{L}$) and Acc is the accumulation rate (mm w.e./yr).

280

Fig. 6 reports the concentrations and fluxes of ssNa^+ , nssCa^{2+} , nssSO_4^{2-} , nssCl^- and NO_3^- in surface snow samples and concentrations mean $\pm 1\sigma$ in the snow pits. These markers are selected to study the spatial variability and deposition processes of the different types of aerosols (ssNa^+ for sea salt aerosol, nssCa^{2+} for crustal aerosol, nssSO_4^{2-} for biogenic aerosol) and species mainly present as gas (HCl and HNO_3) present into the Antarctic atmosphere.

Table 2. Accumulation rates at different sites along the EAIIST traverse



Sampling point	Dist. Indian Ocean (km)	Years of accumulation	Acc. Rate (mm snow/yr)	Acc. Rate (mm we/yr)	References
Dome C	930	1964-1992	80-88	32.8	(Traversi et al., 2009)
Dome C	930	1992-2016	90	35.3	(Caiazza et al., 2021) ²⁹⁰
AGO-5	1165	1992-2019	73.9	25.7	This study
PALEO	1440	1992-2019	63.9	22.6	This study

295 Regarding the comparison between range of concentrations in the snow pit respect to those at the surface two different patterns are visible: (i) ions presenting concentrations in the superficial layer in the range of $\text{mean} \pm 1\sigma$ in the snow pits; these are ssNa^+ , nssCa^{2+} and nssSO_4^{2-} which are considered stable in the snow layers and (ii) ions presenting concentration in the superficial snow samples higher than $\text{mean} + \sigma$ in the snow pits, namely Cl^- (for the sites showing the lowest accumulation rates) and NO_3^- , that are considered reversely deposited species.

300 The concentration pattern of ssNa^+ (and therefore also for the other ions mainly arising from sea spray: K^+ and Mg^{2+}) shows a constant trend in concentrations and a decreasing trend in fluxes as latitude, distance from Dome C and distance to the Indian Ocean increase. Besides, ssNa^+ concentrations measured in this area are in the range of that measured at Dome C (Udisti et al., 2004), Dome Fuji (Iizuka et al., 2006) and in general in the Antarctic Plateau (Bertler et al., 2005).

This different pattern of concentration and fluxes is typical of wet deposited species in low accumulation sites. In this area, the snowflakes contain the same amount of sea salt aerosol in all the sites, as revealed by the snow concentration trend, but in sites with less snowflake falling we observe a lower deposition flux of sea salt aerosol.

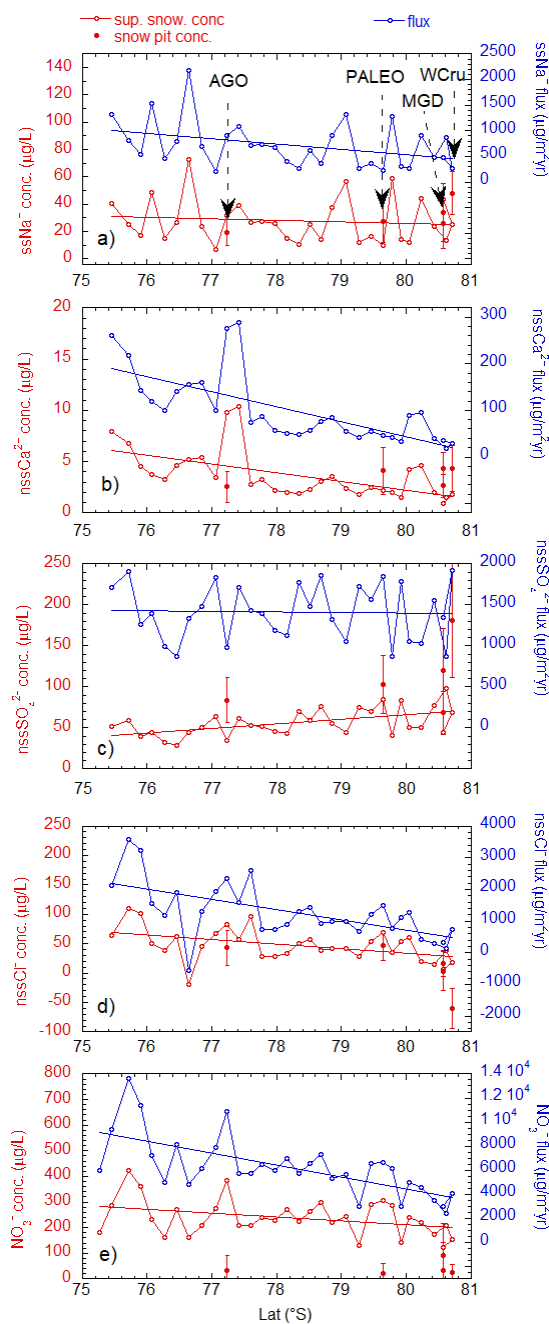


Figure 6. SsNa^+ , nssCa^{2+} , nssSO_4^{2-} , nssCl^- and NO_3^- concentrations (red) and fluxes (blue) in the superficial snow samples (empty dots) and mean $\pm 1\sigma$ concentration in snow pit samples (red dots and vertical lines) as function of latitude (see Fig. 2 and Table 1S for the corresponding increases of distance from Dome C and distance from Indian Ocean). The linear fitting is reported in each plot to highlight the trend.



Crustal aerosol is found to be mainly dry deposited in the inner Antarctic plateau (Albani et al. 2012 and references therein) and, if the crustal aerosol supply to the plateau were constant, its deposition flux should increase moving South from Dome C, due to a progressively lower accumulation rate. On the contrary, a decreasing trend of nssCa^{2+} deposition fluxes as accumulation decreases is evident (Fig. 6b), implying that atmospheric concentration of crustal aerosol decreases along the route from Dome C as latitude increases.

Excluding the sporadic input from volcanic eruptions, the majority of nssSO_4^{2-} found in the snow and aerosol of Antarctica comes from marine biological activity (e.g. Becagli et al. 2022; Kaufmann et al. 2010; Wolff et al. 2006).

Sulfate concentrations measured in this work are of same order of magnitude with respect to those reported for Dome Fuji (Iizuka et al., 2006), Dome C (Udisti et al., 2004) and in general for the Antarctic Plateau (Bertler et al., 2005), but an increasing trend is observed as latitude increases.

Legrand and Mayewski (1997) showed that in low accumulation sites in the inner Antarctic Plateau sulfate is deposited by dry deposition therefore change in concentration in snow layer should be ascribed to a variation in accumulation rate.

Indeed, as above reported a decreasing trend of accumulation rate was observed as the distance from Indian Ocean (and latitude) increases. Considering the sulphate flux it's clear that the amount of nssSO_4^{2-} deposited is constant, indicating almost constant atmospheric concentrations in this area and confirming that dry deposition as main deposition process.

This evidence has an important implication as depositional flux of dry deposition is given by:

$$F = C_{\text{atm}} * v$$

Where C_{atm} is the concentration of nssSO_4^{2-} into the atmosphere and v is the deposition velocity. The deposition velocity depends on the size distribution of the considered species, in addition to the wind speed and relative humidity of the atmosphere. Deposition velocity spans between 0.03 to 0.3 cm/sec for the submicrometric particles (Duce et al. 1991). A previous study of nssSO_4^{2-} in size segregated aerosol at Dome C reveal that nssSO_4^{2-} are mainly distributed in the submicrometric fraction showing an average annual concentration in this fraction of about 30 ng/m^3 (as average for the year from 2005 to 2012, Becagli et al., 2022). Considering this value as the mean annual aerosol concentration and a deposition velocity of 0.15 cm/sec we obtain a mean annual deposition flux of about $1400 \text{ } \mu\text{g/m}^2\text{yr}$ that completely agrees with the value ($1370 \text{ } \mu\text{g/m}^2\text{yr}$) calculated as average of the fluxes arising from nssSO_4^{2-} concentration in the superficial snow collected at each site of the traverse.

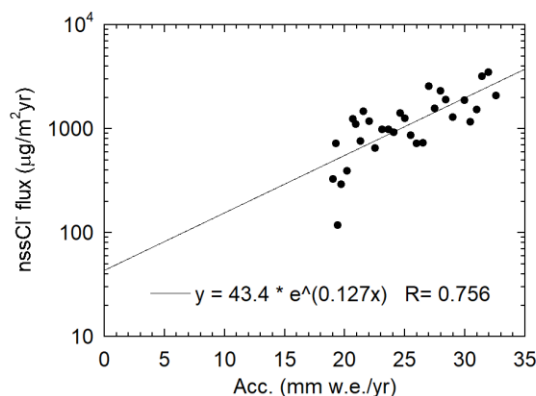
The flux variations around the average values are likely due to different mix of summer and winter snow precipitation collected in the most superficial snow. Indeed, considering the nssSO_4^{2-} concentration measured in mid-summer (85 ng/m^3) and mid-winter (5 ng/m^3) in the aerosol submicrometric fraction at Dome C by Becagli et al. (2022), fluxes change during the year from about $4000 \text{ } \mu\text{g/m}^2 \text{ yr}$ to a minimum of $235 \text{ } \mu\text{g/m}^2$. This evidence demonstrates that atmospheric concentration of nssSO_4^{2-} in the plateau is spatially constant, but obviously it varies seasonally. Moreover, it has been shown that nssSO_4^{2-} flux in EPICA-



Dome C ice core has not significantly changed throughout the last eight glacial cycles, which was interpreted to indicate a non-significant change in marine biogenic activity (Wolff et al., 2006). This conclusion is inconsistent with data derived from marine sediment cores that shows lower productivity at latitudes higher than 50°S during the last glacial period than during the current warm period (Kohfeld et al., 2005) that should reflect a lower flux of nssSO_4^{2-} during glacial. The results achieved by Ishino et al. (2019) by sulfur isotopic measurements may allow explaining this apparent controversial evidence. The Authors found a higher contribution of a non-biogenic source of nssSO_4^{2-} contribution in glacial time than in interglacial, demonstrating that this source is consistent with sulfate crustal input. To estimate the crustal fractions of sulphate, the nssCa^{2+} fluxes were multiplied by the $\text{SO}_4^{2-}/\text{Ca}^{2+}$ ratio in the uppermost Earth crust and (0.592 w/w, Bowen, 1979). The contribution of crustal source is about 10% at sites nearest to Dome C confirming the mean annual value obtained by Ishino et al. (2019) at present day from aerosol measurements. It is interesting to notice that the contribution of the crustal source to nssSO_4^{2-} decreases as latitude increases, making the sites far from Dome C more suitable to infer the past variation of the biogenic activity from nssSO_4^{2-} fluxes.

As above reported, nssCl^- arises from the exchange reactions between chloride in the sea salt aerosol and acidic species such as H_2SO_4 and HNO_3 (reaction 1 and 2). Therefore, the positive value of nssCl^- indicates an extra source of HCl transported and deposited separately respect to unmodified sea salt aerosol. Conversely, if the reaction occurs in the snow layers at the expense of the already deposited sea salt aerosol, nssCl^- are negative. Therefore, the negative values of nssCl^- represent the loss of chloride from snow layers in the form of HCl from Cl^- deposited as NaCl and MgCl (i.e. arising form of sea spray). This is due to the reactions (1) and (2) that moves towards the formation of HCl due to its more volatile nature compared to H_2SO_4 .

In superficial snow concentration and fluxes of nssCl^- show a general decreasing trend with always positive values, demonstrating the presence of HCl in the freshly deposited snow. The decreasing trend as accumulation rate decreases is due to the wet and dry deposition processes both occurring for this species. By reporting the flux as function of accumulation rate an exponential function is found (Fig. 7) where the values for accumulation ratio = 0 is due to the dry deposition. Fig.7 shows that dry deposition accounts for a minor amount of this species being deposited mainly as wet deposition also at sites with low accumulation rate. Another effect leading to a decreasing in nssCl^- concentration as accumulation rate decreases is the post depositional loss of HCl, that can be highlighted by reporting the nssCl^- concentration as function of depth (Fig. 8). Break point analysis was performed at the concentration vs. depth profile for each site aiming to find the depth at which post depositional loss ends and the concentration preserved at the end of reemission processes. A single or none break point was assumed to be present in each profile and its coordinates were computed by means of linear estimation using the “segmented” package in R software (Muggeo, 2003, <https://cran.r-project.org/web/packages/segmented/index.html>). Therefore, the x value of break point coordinates (if found in the depth range of the snow-pit) represents the depth at which end the active layer (active for re-emission processes) and start the archive layer. The y coordinates the archived concentration at the site.



380

Figure 7. Scatter plot of nssCl⁻ flux vs accumulation rate. NssCl⁻ are reported in logarithmic scale, therefore the exponential fitting appears as linear in this plot.

In all the snow-pits a decreasing trend of nssCl⁻ concentration as depth increases is observed, but only at AGO5 the constant concentrations are positive. Therefore, only at this site the deposited HCl partially stays stably fixed in the deep layer. Considering an average value of 100 μg/L of HCl deposited in the superficial layer at AGO5, only the 24% is preserved at depth higher than 1m. At PALEO, MGD-A and MGD-E the decreasing trend of nssCl⁻ do not reach stable values in the depth interval covered by the snow-pit, and negative values (evidencing the chloride depletion of the deposited sea salt aerosol) are reached at depths that are more and more shallow as accumulation rate decreases. A particular trend is visible at WCru (where the negative values are already reached at 10 cm depth and constant negative concentrations of about -70 μg/L are reached at about 60 cm depth. The loss of HCl from sea spray in the most superficial 10 cm is due to the presence of ice already at the surface indicating an older layer than expected considering the snow accumulation layer or rapid ice formation due to the wind scouring. Both processes result to a loss of HCl.

Nitrate is present as acidic species in the atmosphere over the Antarctic Plateau. It is produced by the oxidation of nitrogen oxides (NO_x -> NO + NO₂) coming from the downward transport of NO_x produced by stratospheric sources, the long-range transport of air masses enriched in NO_x by tropical lightning (Legrand and Kirchner, 1990), sedimentation of polar stratospheric clouds (Tritscher et al. 2021), and from the action of the snowpack, which can act both as a source and as an accumulator of HNO₃ and its precursors (Savarino et al. 2007). High concentrations and fluxes are measured in all the superficial snow samples collected along the traverse (fig. 6). Besides, at WCru, MGD-a and MGD-E sites concentration in the first sample of snow pits (representing the most superficial 3 cm layer) are higher than the concentration measured in the superficial snow (representing the most superficial 10 cm layer) (Table 3).

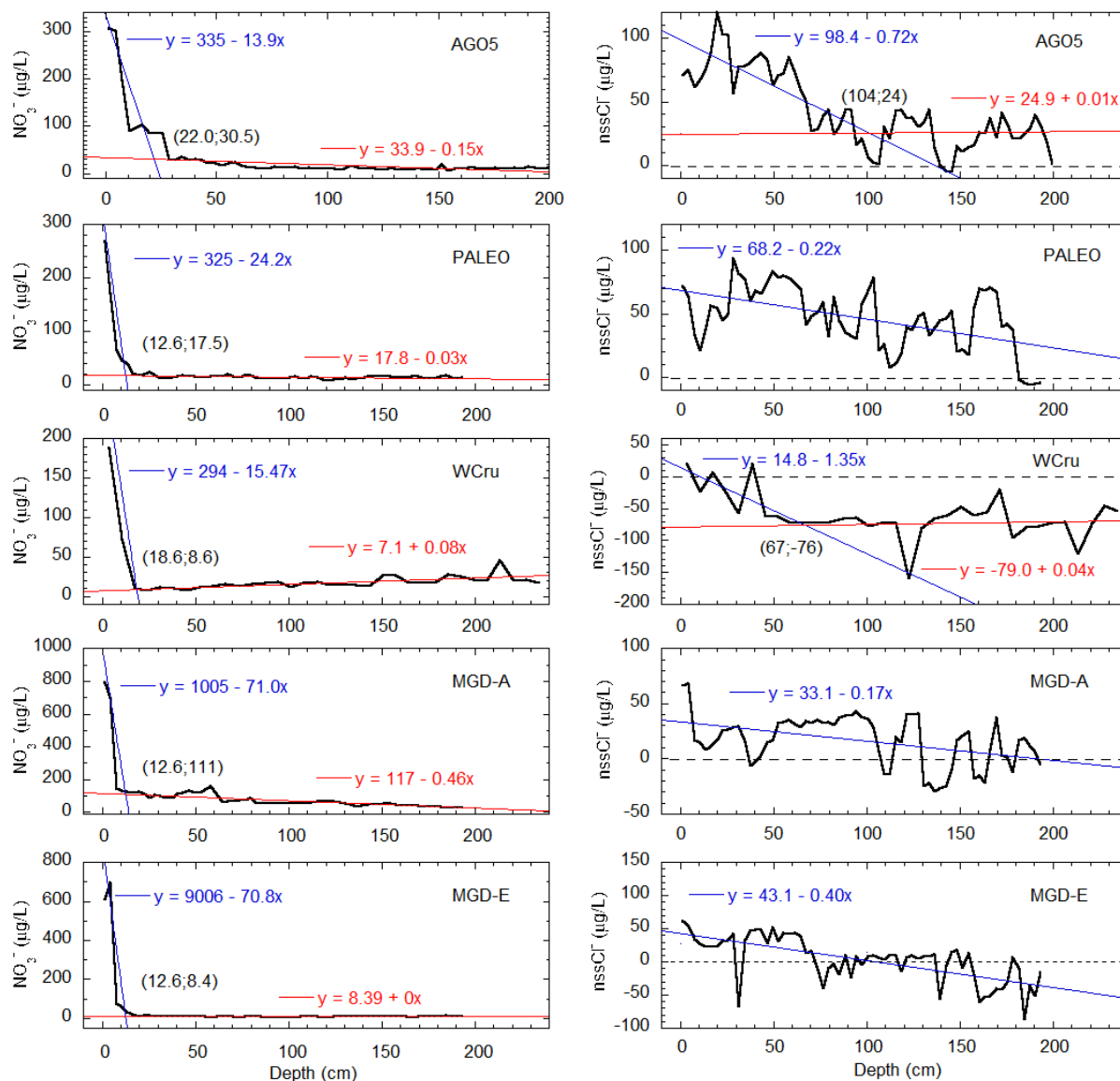


Figure 8. Nitrate and nssCl⁻ concentrations as function of depth in the snow pits dug at AGO-5, PALEO, WCru, MGD-A, and MGD-E. The two linear regressions obtained by the break point analysis are plotted for each site, the coordinates of the lines intersection are reported in each plot (x; y). For nssCl⁻ at PALEO, MGD-A and MGD-E the break point analysis has not statistical significance and the regression lines fitting the data points are not reported. The dashed line at 0 value for nssCl⁻ highlight the presence of HCl (for nssCl⁻>0) and the Chloride depletion from the already deposited sea salt aerosol (nssCl⁻<0).



410 HNO₃ is deposited by scavenging during formation of precipitation, uptake of HNO₃ onto the ice crystal's surface during and
after precipitation and by dry deposition (Röthlisberger et al., 2002). It was demonstrated that in the case of liquid or mixed
clouds, essentially all HNO₃ is removed from the gas phase independent of the cloud temperature (Seinfeld and Pandis, 1998),
conversely the co-condensation of HNO₃ and water molecules on ice crystals would lead to a very low bulk concentration in
the fresh snow (Thibert and Dominé, 1998). Therefore, in the absence of liquid water, i.e. in ice clouds, the high NO₃⁻
415 concentrations found in surface snow could not be explained. The main processes leading to the high concentration in snow
surface are the dry deposition and the uptake on snow crystals. The dry deposition was calculated by the mean atmospheric
HNO₃ measured in December-January at Dome C (Erbland et al., 2013) of about 100 ng/m³ and assuming it as constant in this
area. Literature data report for HNO₃ different values for the dry deposition velocity; for instance, at South Pole station and
DML (which have a similar snow accumulation rate) a value of 0.8 cm/s was used (Huey et al., 2004; Winton et al., 2020).
420 Other estimates of dry deposition velocities include 0.05–0.5 cm/s for HNO₃ over snow (Hauglustaine et al., 1994; Seinfeld
and Pandis, 1998) and a higher value for areas over the open ocean (1.0 cm/s, Duce et al., 1991) due to the size distribution
shifted toward high diameters in this environment. Finally, a deposition velocity of 0.15 cm/s was used for summer HNO₃ at
Dome C (Erbland et al., 2013). The estimated NO₃⁻ deposition velocity at Dome C is low because of the strong recycling of
NO₃⁻ on the polar plateau in summer; i.e. reactive nitrogen is re-emitted from the skin layer to the atmosphere. We assume that
425 the value used by Erbland et al. (2013) could better reflect the deposition velocity in this area, and the value of 0.15 cm/s was
used to calculate the concentration and fluxes due to this process at each site (Table 3). Table 3 shows that the calculated
concentration expected considering only the dry deposition are lower than the measured. This evidence can be due to (i)
considering constant the concentration of NO₃⁻ into the atmosphere and a low deposition velocity; (ii) other deposition
processes (snow uptake) being more efficient as distance from Dome C increases; (ii) post depositional processes occurring in
430 most superficial centimeters of snow.

It is not possible to verify the first issue without measurement of HNO₃ into the atmosphere, but in case the species is only dry
deposited, the trend of snow concentration should show an increase as accumulation rate decreases. Conversely Fig.6e shows
a decreasing trend in concentration, therefore the dry deposition cannot be the only deposition process. The adsorption of
HNO₃ on ice surfaces is temperature dependent with higher uptake at lower temperatures (Abbatt, 1997; Jones et al., 2014).
435 The surface uptake of HNO₃ is estimated using a linear regression through the values for temperature dependent uptake found
by Abbatt (1997) and assuming a typical surface area of 4000 m²/m³ (Narita, 1971). The temperature data (daily maximum and
minimum) are from automated weather stations installed in the Megadune area and at Paleo site during the traverse and derived
by model for the other sites (Casado et al., 2022). Temperature varies daily following maxima and minima of solar radiation,
but there are not large differences among the sites during the time of the traverse (Casado et al., 2022). The calculated
440 concentrations by the snow uptake (table 3) are generally higher than the measured concentrations (also considering the higher
measured temperatures at each site determining a lower uptake), but they reflect the same trend as distance from Dome C
increases. Indeed, at Dome C, AGO5 and PALEO the concentration decreasing trend can be explained by the decreasing
temperature at the beginning of the traverse, lower temperature favoring the uptake by superficial snow. Going forward with



the traverse, min and max temperature remain constant, but as density of snow is decreases, decreases the volume of water
445 containing the surface area of uptake. Indeed, the lower calculated concentration are at WCru and MGD-E where superficial
layer has a higher density due to the ice crystal formation. In the two megadune sites (same temperature, but different
superficial snow density) the measured HNO₃ concentration is higher at MGD-A site with lower snow density. Therefore, the
HNO₃ deposition in summer is a combination of dry deposition and snow uptake, the latter having the potentiality to give
highest concentration in superficial snow.

450 In winter when temperature reach -80°C, the surface uptake is more active, but at this time HNO₃ into the atmosphere is low
(Erbland et al., 2013; Traversi et al., 2014) therefore the main deposition occurs in summer. It is known that HNO₃ is not stably
fixed in the snow and post depositional effect are well documented in sites with low accumulation rate (Savarino et al., 2007;
Traversi et al., 2009; Erbland et al., 2013; Winton et al., 2020, Akers et al., 2022). Post depositional processes occurs in the
455 the first centimeters of snow, isotopic measurements performed at Dome C revealed that in the central Antarctic plateau in summer
the dominant reemission process is photolysis (Erbland et al., 2013). The reemission process occurring in winter when the
absence of UV radiation does not allow the photolysis of HNO₃ are less clear and less documented, but as above reported the
deposition in wintertime is low.

Reporting the NO₃⁻ concentration as function of depth in the 5 snow pits it is possible to quantify the impact of post deposition
processes in term of rate of loss and NO₃⁻ concentration preserved in the snow (Fig. 8).

460 Fig. 8 shows that the re-emission of HNO₃ occurs fast in the most superficial centimetres of snow in all the sampling sites and
it is concluded in 20 cm of deposition at maximum. The background NO₃⁻ concentrations preserved in the snow layer decrease
as the accumulation rate decreases. An apparent exception to this is represented by the pattern observed at MGD-A where the
break point concentration is 111 µg/L (i.e higher than at sites with higher accumulation rate). In this case it has to be noticed
that this concentration is not constant but further decreases as depth increases. Therefore, in this case the actual NO₃⁻
465 concentration preserved at this site is lower than this value and it is not detectable in the depth range covered by the snow pit.
Particular attention has to be paid to the comparison between the two sites in the megadune area: the accumulation site (MGD-
A) presents higher concentration at the surface than MGD-E likely due to the relative position respect to katabatic wind
favouring the snow redistribution at MGD-E, besides the active layer seems to be the same (about 12 cm of snow) but below
this layer at MGD-A the re-emission of HNO₃ is still active, even if less efficient. Another interesting feature is that sites
470 affected by wind erosion (MGD-E) and formation of ice crystals (WCru) present still efficient reemission processes with the
lowest NO₃⁻ concentration (about 8.5 µg/L) preserved in the snow layers (Fig. 8 e Tab. 3).

475



Table 3. Nitrate concentration in superficial and sub-superficial snow layers considered as the concentration stably fixed in several sites in the Antarctic Plateau.

*Accumulation rate for WCru, MGD are evaluated from the regression line as reported in Fig. 9. The sites MGD-A and MGD-E are at the same distance from the Indian Ocean therefore only one accumulation rate is calculated. This value represents an intermediate value between the two sites sampled in magadune area having different accumulation rate. †The reported accumulation rate for Dome C are from 1992-2016 reported in (Caiazza et al., 2021).

Reference	Sampling point	Acc.rate (mm w.e./yr)	Temp. (Max)	Density (kg/L)	Conc. Snow uptake	Conc. Dry dep	Concentration in superficial snow - µg/L (depth of considered layer - cm)	Concentration stably fixed (µg/L) (depth of considered layer - cm)
This study	AGO-5	25.7	-25	0.28	1106	184	307 (0-3cm); 385 (0-10cm)	30.5 (22.0 cm)
This study	PALEO	22.6	-20	0.26	757	209	270 (0-3cm); 304 (0-10cm)	17.5 (12.6cm)
This study	WCru	19.0*	-20	0.37	532	249	188 (0-3cm); 155 (0-10cm)	8.7 (18.6cm)
This study	MGD-A	19.4*	-20	0.28	703	244	793 (0-3cm); 174 (0-10cm)	-
This study	MGD-E		-20	0.35	562	244	607 (0-3cm); 207 (0-10cm)	8.4 (12.6 cm)
Shi et al., 2018	Dome A						350 (0-3cm)	
Udisti et al., 2004	Dome C	35.3 †	-25	0.3	1108	134	381 (0-2cm)	
Traversi et al., 2017	Dome C	35.3 †	0.3	1108	134	0.3	200 (0-2cm); 800 (0-0.5cm)	
Erbland et al., 2013	Dome C	35.3 †	0.3	1108	134	0.3	100 / 600 (0-10cm)	
Iizuka et al., 2006	Dome Fuji							40.3 (0-3.4 m)

485

Given the different efficiency of post-depositional processes and the dependence of NO₃⁻ concentration on accumulation, time of year and depth of the sampled superficial snow layer, a direct comparison with data from other sites is not possible. Table 3 shows data from several studies carried out on snow samples of specified thickness collected in summer and concentration stability fixed in snow layer for each site.

490



5-Conclusions

This paper reports the data of chemical composition and spatial distribution of aerosol chemical markers for unexplored region of the Antarctic Plateau along the EAIIST traverse from Dome C towards the South Pole. The study of the spatial variability of chemical impurities in the snow allows to understand the deposition and post deposition processes of aerosol and gaseous species in sites with very low snow accumulation rate and especially in sites characterized by particular glaciological characteristics such as megadune and wind crust.

The nssSO_4^{2-} arising from biogenic emission is the dominant source of background sulphate, but the volcanic signature of Pinatubo eruption occurred in 1991 and visible at AGO-5 and PALEO allow the determination of accumulation rates that are 25.7 and 22.6 mm of water equivalent/year respectively at the two sites.

The insoluble dust profiles measured at AGO5 and PALEO are both presenting a peak at 61.5-64.5 cm and 37.5-40.5 cm respectively. These peaks are characterised by an increase in the concentration of total dust particle with a mineral dust grain size progressively decreasing. The stratigraphic location of the peak is compatible with deposition of volcanic ash from the Puyehue-Cordón Caulle explosive eruption event of June 2011 also detected in West Antarctica.

Considering the accumulation rate at Dome C (Caiazza et al., 2021; Traversi et al., 2009) and those obtained from AGO-5 and PALEO snow-pits it is possible to highlight a decreasing trend of accumulation rate as the distance from the Indian Ocean increases and considering linear the decreasing trend the accumulation rate and deposition fluxes for the main markers in each superficial snow sampling site was calculated.

The ssNa^+ accounting for the 92.5% of the total Na^+ was chosen as marker of sea spray deposition and it is preserved stably in the snow layers. SsNa shows a constant trend in concentrations (around $30 \mu\text{g}/\text{m}^3$) and a decreasing trend in fluxes as latitude, distance from Dome C and distance to the Indian Ocean increase. This pattern demonstrates that, despite the very low accumulation rate in this area, the main deposition process of sea spray aerosol is the wet deposition.

Conversely, nssSO_4^{2-} sulfate concentration presents an increasing trend as accumulation rate decreases, indeed by calculating the flux of nssSO_4^{2-} it results to be constant along the traverse, but the relative importance of the fluxes of biogenic and crustal sources for nssSO_4^{2-} both dry deposited, change as distance from Dome C increases. This implies that constant atmospheric concentrations of nssSO_4^{2-} in this area arise from different contributions of the two sources with the impact of biogenic source that increases as distance from Dome C increases. The presence and quantification (by nssCa^{2+}) of a dry deposited crustal source as the biogenic one provides a further evidence of previous findings based on isotopic measurement of S in the nssSO_4^{2-} (Ishino et al., 2019) and sheds light on the paradox of constant biogenic activity during glacial and interglacial time as Antarctic ice core seems to show (Wolff et al., 2006), on the contrary of marine sediment cores (Kohfeld et al., 2005). Indeed, the measured constant fluxes of nssSO_4^{2-} in glacial and interglacial periods do not mean that biogenic source (and therefore the biogenic activity in the Antarctic Ocean) is constant; in fact, during the glacial time the crustal source of nssSO_4^{2-} increases, meaning that the biogenic nssSO_4^{2-} decreases, thus indicating a reduced biogenic productivity respect to interglacial time.



525 NssCl^- represent the fraction of Cl^- deposited as HCl and arises from the exchange reactions between chloride in the sea salt aerosol and acidic species such as H_2SO_4 and HNO_3 . If these reactions occur in the atmosphere, HCl is transported and deposited separately respect to unmodified sea salt aerosol. HCl is deposited by wet deposition but it undergoes post depositional processes that are more evident as accumulation rate is lower and especially in sites affected by wind crust formation. In these sites a Chloride depletion (negative value of nssCl^-) is already shown in the first 10 cm of snow. Cl^- depletion is due to the reemission into the atmosphere of HCl deposited as sea salt by the exchange reaction with H_2SO_4 .

530 Another important marker in ice core is HNO_3 , it is deposited mainly in summer both by dry deposition and especially by superficial snow uptake (the lower is the temperature the higher is the uptake), but it is reversibly deposited. Previous study revealed that the main reemission process in summer is HNO_3 photolysis (Erbland et al., 2013), but snow redistribution processes seem to have a role in determining the concentration in the superficial snow. Indeed, by comparing accumulation and ablation sites at MGD the highest concentration on the most superficial 3 cm of snow is measured in the accumulation site
535 (MGD-A). Besides, among all the sites the lowest values in the superficial snow layer are measured at WCru, the site most affected by wind scouring.

Break point analysis applied on HNO_3 concentration vs depth profile allow to establish the depth of the active layer and the concentration of NO_3^- stably preserved in the snow in each site. The depth of the active layer is very low and span from 22 cm to 12 cm and concentration preserved in the snow decreases as the accumulation rate decreases, the lower concentration is
540 preserved at WCru and MGD-E (8.5 $\mu\text{g/L}$) showing again that wind scouring play a role in the re-emission processes in the active layer.

The knowledge and quantification of all the above reported processes will allow the interpretation of the ice core stratigraphies as function of environmental and climatic variation in the past. Besides, some processes that are visible in the shallow snow layers at sites characterized for instance by ice crust formation, can be considered as analogous of those occurring in the deepest
545 snow layers. The knowledge of such processes may allow interpreting the ice core stratigraphy in low accumulation site likely recording, at selected sites, the climate history of more than one million years ago (Wolff et al., 2022).

References

- Abbatt, J. P. D.: Interaction of HNO_3 with water-ice surfaces at temperatures of the free troposphere. *Geophys. Res. Lett.*,
550 24(12),1479-1482. 1997.
- Akers, P. D., Savarino, J., Caillon, N., Servettaz, A. P. M. , Le Meur, E., Magand, O., Martins, J., Agosta, C., Crockford, P., Kobayashi, K., Hattori, S., Curran, M., van Ommen, T., Jong, L., Roberts, J. L.: Sunlight-driven nitrate loss records Antarctic surface mass balance. *Nature Communication*, 13(4274), 1-10.. 2022.



- Albani, S., Mahowald, N.M., Delmonte, B. et al. Comparing modeled and observed changes in mineral dust transport and
555 deposition to Antarctica between the Last Glacial Maximum and current climates. *Clim Dyn* 38, 1731–1755 (2012).
<https://doi.org/10.1007/s00382-011-1139-5>.
- Becagli, S., Marchese, C., Caiazza, L., Ciardini, V., Lazzara, L., Mori, G., Nuccio, C., Scarchilli, C., Severi M., Traversi, R.:
Biogenic aerosol in central East Antarctic Plateau as a proxy for the ocean/atmosphere interaction, *Sci. Tot. Environ.*, 810,
151285, 2022.
- 560 Becagli, S., Proposito, M., Benassai S., Flora, O., Genoni, L., Gragnani, R., Largiuni, O., Pili, S. L., Severi, M., Stenni, B.,
Traversi R., Udisti R., and Frezzotti M.: Chemical and isotopic snow variability in East Antarctica along the 2001/02 ITASE
Traverse, *Ann. Glaciol.*, 39, 473–82, <https://doi.org/10.3189/172756404781814636>, 2004.
- Becagli, S., Proposito, M., Benassai, S., Gragnani, R., Magand, O., Traversi, R., and Udisti, R.: Spatial distribution of biogenic
sulphur compounds (MSA, NssSO₄²⁻) in the Northern Victoria Land–Dome C–Wilkes Land Area, East Antarctica, *Ann.*
565 *Glaciol.*, 41, 23–31, <https://doi.org/10.3189/172756405781813384>, 2005.
- Benassai, S., Becagli S., Gragnani R., Magand O., Proposito M., Fattori I., Traversi R., and Udisti R.: Sea-Spray Deposition
in Antarctic Coastal and Plateau Areas from ITASE Traverses, *Ann. Glaciol.*, 41, 32–40,
<https://doi.org/10.3189/172756405781813285>, 2005.
- Bertler, N., et al: Snow chemistry across Antarctica, *Ann. Glaciol.*, 41, 167–79. <https://doi.org/10.3189/172756405781813320>,
570 2005.
- Bowen, H. J. M. *Environmental Chemistry of the Elements*. Academic Press, 1979.
- Caiazza, L., Becagli, S., Bertinetti, S., Grotti, M., Nava, S., Severi, M., and Traversi, R.: High resolution chemical
stratigraphies of atmospheric depositions from a 4 m depth snow pit at Dome C (East Antarctica), *Atmosphere* 12(7). doi:
10.3390/atmos12070909, 2021.
- 575 Casado, M., Leroy-Dos Santos, C., Fourré, E., Favier, V., Agosta, C., Arnaud, L., Prié, F., Akers, P. D., Janssen, L., Kittel, C.,
Savarino, J., and Landais, A.: Water vapor isotopic signature along the EAIIST traverse, EGU General Assembly 2022, Vienna,
Austria, 23–27 May 2022, EGU22-13362, <https://doi.org/10.5194/egusphere-egu22-13362>, 2022.
- Castellano, E., Becagli, S., Hansson, M., Hutterli, M., Petit, J. R., Rampino, M. R., Severi, M., Steffensen, J. P., Traversi, R.,
and Udisti, R.: Holocene volcanic history as recorded in the sulfate stratigraphy of the European project for ice coring in
580 Antarctica Dome C (EDC96) ice core, *J. Geophys. Res. D: Atmospheres* 110(6), 1–12. <https://doi.org/10.1029/2004JD005259>.
2005.
- Cole-Dai, J., and Mosley-Thompson, E.: The Pinatubo eruption in South Pole snow and its potential value to ice-core
paleovolcanic records, *Ann. . Glaciol.*, 29, 99–105, <https://doi.org/10.3189/172756499781821319>, 1999.
- Dahe, Q., Zeller, E. J., and Dreschhoff, G. A. M.: The Distribution of nitrate content in the surface snow of the Antarctic ice
585 sheet along the route of the 1990 International Trans-Antarctica Expedition, *J. Geophys. Res.*, 97(A5), 6277,
<https://doi.org/10.1029/92ja00142>, 1992.



- Delmonte B., Petit J. R., Andersen K. K., Basile-Doelsch I., Maggi V., Ya Lipenkov, V.: Dust size evidence for opposite regional atmospheric circulation changes over east Antarctica during the last climatic transition, *Clim. Dyn.*, 23, 427–438, <https://doi.org/10.1007/s00382-004-0450-9>, 2004.
- 590 Delmonte, B., Andersson, P. S., Schöberg, H., Hansson, M., Petit, J. R., Delmas, R., Gaiero, D. M., Maggi, V., and Frezzotti M.: Geographic provenance of aeolian dust in East Antarctica during Pleistocene glaciations: preliminary results from Talos Dome and comparison with East Antarctic and New Andean ice core data, *Quaternary Sci. Rev.*, 29(1–2), 256–64, <https://doi.org/10.1016/j.quascirev.2009.05.010>, 2010.
- Dixon, D. A., Mayewski, P. A., Korotkikh, E., Sneed, S. B., Handley, M. J., Introne, D. S., and Scambos, T. A.: Variations in snow and firn chemistry along US ITASE Traverses and the effect of surface glazing, *The Cryosphere*, 7(2), 515–35, <https://doi.org/10.5194/tc-7-515-2013>, 2013.
- 595 Duce R. A., Liss, P., Merrill, J., Atlas, E., Buat-Menard, P., et al.: The atmospheric input of trace species to the world ocean, *Global Biogeochemical Cycles*, 5(3), 193–259, <https://doi.org/10.1029/91GB01778>, 1991.
- Erbland, J., Vicars, W. C., Savarino, J., Morin, S., Frey, M. M., Frosini, D., Vince, E., and Martins, J. M. F.: Air-snow transfer of nitrate on the East Antarctic Plateau - Part 1: Isotopic evidence for a photolytically driven dynamic equilibrium in summer, *Atmos. Chem. Phys.*, 13(13), 6403–19, <https://doi.org/10.5194/acp-13-6403-2013>. 2013.
- 600 Frezzotti, M., Gandofi, S., Urbini, S.: Snow megadunes in Antarctica: sedimentary structure and genesis, *J. Geophys. Res.*, 107(D18), 4344, <https://doi.org/10.1029/2001JD000673>, 2002.
- Hauglustaine, D. A., Granier C., Brasseur G. P. and Mégie G.: The importance of atmospheric chemistry in the calculation of radiative forcing on the climate system. *J. Geophys. Res.*, 99(D1), 1173–1184. 1994.
- 605 Huey, L. G., Tanner, D. J., Slusher, D. L., Dibb, J. E., Arimoto, R., Chen, G., Davis, D., Buhr, M. P., Nowak, J. B., Mauldin III, R. L., Eisele, F. L., and Kosciuch, E.: CIMS measurements of HNO₃ and SO₂ at the South Pole during ICAT 2000, *Atmos. Environ.*, 38, 5411–5421, doi:10.1016/j.atmosenv.2004.04.037, 2004.
- Iizuka, Y., Hondoh T., and Fujii Y.: Na₂SO₄ and MgSO₄ salts during the Holocene period derived by high-resolution depth analysis of a Dome Fuji ice core, *J. of Glac.*, 52(176), 58–64, <https://doi.org/10.3189/172756506781828926>. 2006.
- 610 Ishino, S., Hattori, S., Savarino, J., Legrand, M., Albalat, E., Albarede, F., Preunkert, S., Jourdain, B., Yoshida N.: Homogeneous sulfur isotope signature in East Antarctica and implication for sulfur source shifts through the last glacial-interglacial cycle. *Scientific Reports*, 9(12378), 1–8. <https://doi.org/10.1038/s41598-019-48801-1>. 2019.
- Jones, A. E., Brough, N., Anderson, P. S., and Wolff, E. W.: HO₂NO₂ and HNO₃ in the coastal Antarctic winter night: a “lab-in-the-field” experiment, *Atmos. Chem. Phys.*, 14, 11843–11851, <https://doi.org/10.5194/acp-14-11843-2014>, 2014.
- 615 Jourdain, B., and Legrand, M.: Year-round records of bulk and size-segregated aerosol composition and HCl and HNO₃ levels in the Dumont d’Urville (Coastal Antarctica) atmosphere: implications for sea-salt aerosol fractionation in the winter and summer, *J. of Geophys. Res. Atmos.*, 107(22), 1–13, <https://doi.org/10.1029/2002JD002471>, 2002.



- Kaufmann, P., Fundel, F., Fischer, H., Bigler, M., Ruth, U., Udisti, R., Hansson, M., de Angelis, M., Barbante, C., Wolff, E.
620 W., Hutterli, M., and Wagenbach, D.: Ammonium and non-sea salt sulfate in the EPICA ice cores as indicator of biological
activity in the Southern Ocean, *Quat. Sci. Rev.*, 29,(1–2), 313–323, <https://doi.org/10.1016/j.quascirev.2009.11.009>, 2010.
- Kerminen, V. M., Teinilä, K., Hillamo R.: Chemistry of sea-salt particles in the summer Antarctic atmosphere, *Atmos.
Environ.*, 34(17), 2817–2825, [https://doi.org/10.1016/S1352-2310\(00\)00089-3](https://doi.org/10.1016/S1352-2310(00)00089-3). 2000.
- Khodzher, T. V., Golobokova, L. P., Osipov, E. Y., Shibaev, Y. A., Lipenkov, V. Y., Osipova, O. P., Petit J. R.: Spatial-
625 temporal dynamics of chemical composition of surface snow in East Antarctica along the Progress station-Vostok station
transect, *Cryosphere*, 8(3), 931–39, <https://doi.org/10.5194/tc-8-931-2014>, 2014.
- Koffman, B. G., Dowd, E. G., Osterberg, E. C., Ferris, D. G., Hartman, L. H., Wheatley, S. D., Kurbatov A. V., Wong, G. J.,
Markle, B. R., Dunbar, N. W., Kreutz, K. J., Yates, M.: Rapid transport of ash and sulfate from the 2011 Puyehue-Cordón
Caulle (Chile) eruption to West Antarctica, *J. Geophys. Res. Atmos.*, 122, 8908–8920, <https://doi.org/10.1002/2017JD026893>,
630 2017.
- Kohfeld, K. E., Le Quere, C., Harrison, S. P. & Anderson, R. F. Role of marine biology in glacial-interglacial CO₂ cycles.
Science 308, 74–78, <https://doi.org/10.1126/science.1105375>.2005-
- Legrand, M. R., and Delmas R. J.: Formation of HCl in the Antarctic atmosphere, *J. Geophys. Res. Atmospheres*, 93(D6),
7153–68, <https://doi.org/10.1029/JD093iD06p07153>, 1988.
- 635 Legrand, M., and Delmas R. J.: Spatial and temporal variations of snow chemistry in Terre Adélie (East Antarctica), *Ann. of
Glaciol.* 7, 20–25, <https://doi.org/10.1017/s0260305500005851>, 1985.
- Legrand, M., and Delmas, R. J.: The ionic balance of Antarctic snow: a 10-year detailed record, *Atmos. Environ.*, 18(9), 1867–
1874, [https://doi.org/10.1016/0004-6981\(84\)90363-9](https://doi.org/10.1016/0004-6981(84)90363-9), 1984.
- Legrand, M., and Mayewski, P.: Glaciochemistry of polar ice cores: a review, *Rev. of Geophys.*, 35(3), 219–243,
640 <https://doi.org/10.1029/96RG03527>, 1997.
- Legrand, M., Preunkert, S., Wolff ,E., Weller, R., Jourdain, B., and Wagenbach, D.: Year-round records of bulk and size-
segregated aerosol composition in central Antarctica (Concordia Site) - Part 1: fractionation of sea-salt particles, *Atmos. Chem.
and Phys.*, 17(22),14039–54, <https://doi.org/10.5194/acp-17-14039-2017>. 2017.
- Li, C., Xiao C., Shi G., Ding M., Dahe, Q., Ren J.: Spatial and temporal variability of marine-origin matter along a transect
645 from Zhongshan Station to Dome A, Eastern Antarctica, *J. Environ. Sci.*, 46, 190–202,
<https://doi.org/10.1016/j.jes.2015.07.011>, 2016.
- McInnes, L. M., Covert, D. S., Quinn, P. K., Germani, M. S.: Measurements of chloride depletion and sulfur enrichment in
individual sea-salt particles collected from the remote marine boundary Layer, *J. Geophys. Res.*, 99(D4), 8257–68,
<https://doi.org/10.1029/93JD03453>, 1994.
- 650 Muggeo, V. M. R.: Estimating regression models with unknown break-points, *Stat. in Medicine*, 22(19), 3055–3071,
<https://doi.org/10.1002/sim.1545>, 2003.



- Mulvaney, R., and Wolff, E. W.: Spatial variability of the major chemistry of the Antarctic ice sheet.” *Ann. Glaciol.*, 20, 440–47, <https://doi.org/10.3189/1994aog20-1-440-447>, 1994.
- Narcisi, B., Petit, J. R., Delmonte, B., Batanova, V., Savarino, J.: Multiple sources for tephra from AD 1259 volcanic signal in Antarctic ice cores, *Quat. Sci. Rev.*, 210, 164–174, <https://doi.org/10.1016/j.quascirev.2019.03.005>, 2019.
- Nardin, R., Amore, A., Becagli, S., Caiazzo, L., Frezzotti, M., Severi, M., Stenni, B., and Traversi, R.: Volcanic fluxes over the last millennium as recorded in the GV7 ice core (Northern Victoria Land, Antarctica), *Geosciences*, 10(1), 1–15, <https://doi.org/10.3390/GEOSCIENCES10010038>. 2020.
- Narita, H.: Specific surface of deposited snow. II. *Low Temp. Sci., Ser. A*, 29, 69–79. [In Japanese with English summary. 1971
- 660 Legrand M. and Kirchner, S.: Origins and variations of nitrate in south polar precipitation, *J. Geophys. Res. Atmosphere*, 95, 3493–3507, <https://doi.org/10.1029/JD095iD04p03493>, 1990.
- Proposito, M., Becagli, S., Castellano, E., Flora, O., Genoni, L., Gragnani, R., Stenni, B., Traversi, R., Udisti, R., and Frezzotti, M.: Chemical and isotopic snow variability along the 1998 ITASE Traverse from Terra Nova Bay to Dome C, East Antarctica, *Ann. of Glaciol.*, 35, 187–94, <https://doi.org/10.3189/172756402781817167>, 2002.
- 665 Röthlisberger, R., Mulvaney R., Wolff E. W., Hutterli M. A., Bigler M., Sommer S., Jouzel J.: Dust and sea salt variability in central East Antarctica (Dome C) over the last 45 kyrs and its implications for southern high-latitude climate, *Geophys. Res. Lett.*, 29(20), <https://doi.org/10.1029/2002GL015186>, 2002.
- Savarino, J., Kaiser, J., Morin, S., Sigman, D. M., Thiemens, M. H.: Nitrogen and oxygen isotopic constraints on the origin of atmospheric nitrate in coastal Antarctica, *Atmos. Chem. Phys.*, 7(8), 1925–45, <https://doi.org/10.5194/acp-7-1925-2007>, 2007.
- 670 Scarchilli, C., Frezzotti, M., Ruti, P. M.: Snow precipitation at four ice core sites in East Antarctica: provenance, seasonality and blocking factors, *Clim. Dyn.*, 37(9–10), 2107–25, <https://doi.org/10.1007/s00382-010-0946->, 2011.
- Severi, M., Becagli, S., Castellano, E., Morganti, A., Traversi, R., Udisti, R., Ruth, U., Fischer, H., Huybrechts, P., Wolff, E., Parrenin, F., Kaufmann, P., Lambert, F., and Steffensen, J. P.: Synchronisation of the EDML and EDC ice cores for the Last 52 Kyr by volcanic signature matching, *Clim. of the Past*, 3(3), 367–74, <https://doi.org/10.5194/cp-3-367-2007>, 2007.
- 675 Shi, G., Hastings, M. G., Yu, J., Ma, T., Hu, Z., An, C., Li, C., Ma, H., Jiang, S., Li, Y.: Nitrate deposition and preservation in the snowpack along a traverse from coast to the ice sheet summit (Dome A) in East Antarctica.” *Cryosphere*, 12(4), 1177–94, <https://doi.org/10.5194/tc-12-1177-2018>, 2018.
- Shi, G., Ma, H., Hu, Z., Chen, Z., An, C., Jiang, S., Li, Y., Ma, T., Yu, J., Wang, D., Lu, S., Sun, B., Hastings, M. G.: Spatial and temporal variations in surface snow chemistry along a traverse from coastal East Antarctica to the ice sheet summit (Dome
- 680 A), *Cryosphere*, 15(2), 1087–95, <https://doi.org/10.5194/tc-15-1087-2021>. 2021.
- Sodemann, H., and Stohl, A.: Asymmetries in the moisture origin of Antarctic precipitation, *Geophys. Res. Lett.*, 36(22), 1–5, <https://doi.org/10.1029/2009GL040242>. 2009.
- Sommer, C. G., Wever, N., Fierz, C., and Lehning, M.: Investigation of a wind-packing event in Queen Maud Land, Antarctica, *The Cryosphere*, 12, 2923–2939, <https://doi.org/10.5194/tc-12-2923-2018>.



- 685 Seinfeld, J. H. and S. N. Pandis. Atmospheric chemistry and physics: from air pollution to climate change. New York, John Wiley and Sons. 1998.
- Suzuki, T., Iizuka, Y., Matsuoka, K., Furukawa, T., Kamiyama, K., Watanabe, O.: Distribution of sea salt components in snow cover along the traverse route from the coast to Dome Fuji Station 1000 km inland at East Dronning Maud Land, Antarctica, *Tellus, Series B: Chem. and Phys. Meteor.*, 54(4), 407–11, <https://doi.org/10.1034/j.1600-0889.2002.201362.x>, 2002.
- 690 Thibert, E. and Dominé F.: Thermodynamics and kinetics of the solid solution of HNO₃ in ice. *J. Phys. Chem., Ser. B*, 102, 4432–4439. 1998.
- Traversa, G., Fugazza, D., and Frezzotti, M.: Megadunes in Antarctica: migration and characterization from remote and in situ observations, *The Cryosphere*, 17, 427–444, <https://doi.org/10.5194/tc-17-427-2023>, 2023.
- Traversi R., Udisti R., Frosini D., Becagli S., Ciardini V., Funke B., Lanconelli C., Petkov B., Scarchilli C., Severi M., Vitale
- 695 V.: Insights on nitrate sources at Dome C (East Antarctic Plateau) from multi-year aerosol and snow records. *Tellus B*, 66, 22550, <http://dx.doi.org/10.3402/tellusb.v66.22550>. 2014.
- Traversi, R., Becagli, S., Brogioni, M., Caiazzo, L., Ciardini, V., Giardi, F., Legrand, M., Macelloni, G., Petkov, B., Preunkert, S., Scarchilli, C., Severi, M., Vitale, V., and Udisti, R.: Multi-year record of atmospheric and snow surface nitrate in the central Antarctic plateau.” *Chemosphere*, 172, 341–54, <https://doi.org/10.1016/j.chemosphere.2016.12.143>, 2017.
- 700 Traversi, R., Becagli, S., Castellano, E., Cerri, O., Morganti, A., Severi, M., Udisti, R.: Study of Dome C site (East Antarctica) variability by comparing chemical stratigraphies, *Microc. J.*, 92(1), 7–14, <https://doi.org/10.1016/j.microc.2008.08.007>. 2009.
- Traversi, R., Becagli, S., Castellano, E., Largiuni, O., Migliori, A., Severi, M., Frezzotti, M., Udisti, R.: Spatial and temporal distribution of environmental markers from coastal to plateau areas in Antarctica by firn core chemical analysis, *Int. J. Environ. Anal. Chem.* 84(6–7), 457–70, <https://doi.org/10.1080/03067310310001640393>, 2004.
- 705 Tritscher, I., Pitts, M. C., Poole, L. R., Alexander, S. P., Cairo, F., Chipperfield, M. P., Grooß, J. U., Höpfner, M.I., Lambert, A., Luo, B., Molleker, S., Orr, A., Salawitch, R., Snels, M., Spang, R., Woiwode, W., Peter, T.: Polar stratospheric clouds: satellite observations, processes, and role in ozone depletion, *Rev. of Geophys.*, 59(2), 1–81, <https://doi.org/10.1029/2020RG000702>, 2021.
- Udisti, R., Becagli, S., Benassai, S., Castellano, E., Fattori, I., Innocenti, M., Migliori, A., Traversi, R.: Atmosphere-snow
- 710 interaction by a comparison between aerosol and uppermost snow-layers composition at Dome C, East Antarctica, *Ann. of Glaciol.*, 39(Ic), 53–61, <https://doi.org/10.3189/172756404781814474>, 2004.
- Udisti, R., Dayan, U., Becagli, S., Busetto, M., Frosini D., Legrand, M., Lucarelli, F., Preunkert, S., Severi, M., Traversi, R., and Vitale, V.: Sea spray aerosol in central Antarctica. Present atmospheric behaviour and implications for paleoclimatic reconstructions, *Atmos. Environ.*, 52, 109–20, <https://doi.org/10.1016/j.atmosenv.2011.10.018>, 2012
- 715 Uemura, R., Masaka, K., Fukui, K., Iizuka, Y., Hirabayashi, M., Motoyama, H.: Sulfur isotopic composition of surface snow along a latitudinal transect in East Antarctica.” *Geophys. Res. Lett.*, 43(11), 5878–85, <https://doi.org/10.1002/2016GL069482>, 2016.



Wolff, E. W., Fischer, H., Fundel, F., Ruth, U., Twarloh, B., Littot, G. C., Mulvaney, R., Röthlisberger, R., De Angelis, M.,
Boutron, C. F., Hansson, M., Jonsell, U., Hutterli, M. A., Lambert, F., Kaufmann, P., Stauffer, B., Stocker, T. F., Steffensen,
720 J. P., Bigler, M., Siggaard-Andersen, M. L., Udisti, R., Becagli, S., Castellano, E., Severi, M., Wagenbach, D., Barbante, C.,
Gabrielli, P., and Gaspari, V.: Southern Ocean Sea-Ice Extent, Productivity and Iron Flux over the Past Eight Glacial Cycles,
Nature, 440(7083), 491–96, <https://doi.org/10.1038/nature04614>, 2006.

Wolff, E. W., Fischer, H., van Ommen, T., and Hodell, D. A.: Stratigraphic templates for ice core records of the past 1.5 Myr,
Clim. Past, 18, 1563–1577, <https://doi.org/10.5194/cp-18-1563-2022>, 2022.

725 Winton, V. H. L., Ming, A., Caillon, N., Hauge, L., Jones, A. E., Savarino, J., Yang, X., and Frey, M. M.: Deposition, recycling,
and archival of nitrate stable isotopes between the air–snow interface: comparison between Dronning Maud Land and Dome
C, Antarctica, Atmos. Chem. Phys., 20, 5861–5885, <https://doi.org/10.5194/acp-20-5861-2020>, 2020.

Data availability

730 Data set is available on PANGAEA at <https://issues.pangaea.de/browse/PDI-34759> and on request at the corresponding author.

Founding

This study was founded by the ANR EAIIST (grant ANR-16-CE01-0011), of the French Agence Nationale de la Recherche,
the BNP-Paribas foundation and its Climate Initiative Program, the Institut Polaire Français IPEV, the MIUR (Ministry of
735 Education, University and Research) through the PNRA (National Antarctic Research Program) EAIIST project (grant
PNRA16_00049-B) and PRIN2017 project “Innovative Analytical Methods to study biogenic and anthropogenic proxies in
Ice COres” AMICO (grant PRIN_2017EZNJWN_006).

Author contributions.

740 SiB, RT and MB conceived and conceptualized the idea. The IC measurements were carried out by SV, SaB and RN with the
supervision of MS. Dust measurements were carried out by CA, BD. The samples were collected by AS, JS. Sampling site
strategy was developed by MF and JS. All authors contributed to the data analysis and interpretation of the results. SV, SaB
and SiB wrote the paper, using feedback from all other co-authors.

745 Acknowledgements

The authors would like to warmly thank all the participants of the EAIIST traverses for their hard field contributions allowing
the collection of the crucial in-situ measurements used in this study.